Journal of Catalysis 257 (2008) 307–314

Contents lists available at ScienceDirect

Journal of Catalysis

www.elsevier.com/locate/jcat

Morphology changes induced by strong metal–support interaction on a Ni–ceria catalytic system

Victor M. Gonzalez-DelaCruz, Juan P. Holgado, Rosa Pereñíguez, Alfonso Caballero *

Instituto de Ciencia de Materiales de Sevilla (CSIC-University of Seville), Departamento de Química Inorganica, Universidad de Sevilla, Avda. Américo Vespucio, 49, 41092 Seville, Spain

ARTICLE INFO

Article history:
Received 21 March 2008
Revised 7 May 2008
Accepted 12 May 2008
Available online 12 June 2008

Keywords:
Nickel
Ceria
In situ XAS
EXAFS
XANES
APPES
Methane reforming
SMSI

ABSTRACT

The state of the nickel in a Ni/CeO_2 catalyst during hydrogen reduction, steam and dry reforming of methane, have been studied by means of in situ XAS spectroscopy. The catalyst was prepared by a combustion method and, after calcination, very small (about 10 nm) and homogeneous cubic particles of NiO are formed. Once reduced in hydrogen at high temperature (750 °C), the catalyst is active in both steam and dry reforming reactions of methane, but much more stable for the dry reforming reaction. In situ XAS analysis reveals that under reaction conditions at high temperature, the nickel remains completely reduced to Ni(0). However, under strongly reducing conditions (hydrogen or dry reforming at 750 °C), the Ni *K*-edge X-ray absorption spectrum undergoes unexpected modifications that, according to the parameters obtained by fitting analysis, come from changes in the size and morphology of nickel particles, which are now flattened and strongly stabilized on the partially reduced ceria surface. These morphology changes reflect a kind of strong metal–support interaction (SMSI), and could account for the higher stability observed for the dry reforming reaction. The flattened particles are not stable after cooling down to room temperature in hydrogen, while the coke deposited during the dry reforming reaction seems to block the particles, which partially remain even after cooling down to room temperature.

1. Introduction

The steam reforming of methane is at present one of the most important industrial reactions. Not just for obtaining hydrogen [1,2], proclaimed as the fuel of the future economy [3,4], but also for obtaining synthesis gas (CO/H_2) which, in different proportions, is extensively used in industrial processes as methanol synthesis, ammonia synthesis, hydrogenations or Fischer–Tropsch reactions [5]. Besides the steam reforming, the study of dry reforming of methane, using carbon dioxide as oxidant, is of great interest. Even though it has been pointed out as impractical for commercial hydrogen generation [6], it remains as an important process for basic research or as a process to eliminate CO_2 emissions from natural gas deposits. The inexpensive Ni/Al_2O_3 is the catalysts most extensively used for these processes, although its deactivation by carbon formation maintains an important research activity in order to improve the whole processes [7].

Ceria as a support can be a good candidate to improve the catalytic performance of nickel in these reforming reactions, not only by its well-known interesting redox-properties, but also because the support can modify the properties of metals deposited on it by strong metal–support interaction (SMSI) [8,9]. However, only very recently has received attention for this reaction, proving that exhibits good activity and stability under methane reforming reaction [10,11].

In this research, we have prepared a Ni/CeO_2 catalyst by the combustion method, studying its behaviour in the steam and dry reforming of methane. The use of in situ techniques, as XAS and the new APPES spectroscopy, has allowed us to monitor the physico-chemical state of the nickel particles during reaction at high temperature. Some important clues about the evolution of the metallic phase with the different treatments have been elucidated.

2. Experimental

2.1. Catalyst preparation

Ni–ceria system was prepared by combustion synthesis [12]. An aqueous solution containing $Ce(NO_3)_3{\cdot}6H_2O$ and $Ni(NO_3)_2{\cdot}6H_2O$ (from Aldrich) as metal precursors and citric acid as fuel were first evaporated at 200 °C. After heating the solid mixture to 500 °C, an auto-ignited explosive reaction occurs. After cooling down to room temperature (RT), the solid was calcined in synthetic air at 750 °C,

* Corresponding author.
E-mail address: caballero@us.es (A. Caballero).

0021-9517/$ – see front matter
doi:10.1016/j.jcat.2008.05.009

that assuring that no carbonaceous residues remain in the sample. The final product had a composition of 26 wt% Ni/CeO_2.

2.2. X-ray photoemission spectroscopy (XPS)

Conventional XPS spectra were recorded in a LHS-10 Leybold Heraus Spectrometer, with a base pressure of 3×10^{-10} Torr, working in constant pass energy mode (40 eV). Mg$K\alpha$ ($h\nu = 1253.6$ eV) was used as excitation radiation. Calibration of spectra was done on spurious C 1s peak, fixing it at a value of 284.5 eV.

2.3. Temperature-programmed reduction (TPR)

TPR experiments were done on a H_2/Ar mixture (5% H_2, 50 ml/min flow) from room temperature up to 750 °C, with a heating rate of 10 K/min. The experimental conditions were chosen to assure that no peak coalescence occurs [13]. A thermal conductivity detector (TCD), previously calibrated using CuO, and a mass spectrometer in line with the TCD, calibrated with reference mixtures, were used to detect variations of H_2 concentration, and possible sub-products formation.

2.4. Scanning electron microscopy (SEM) and X-ray diffraction (XRD)

SEM images were obtained in a Hitachi S-5200 microscopy, with a field emission filament, using an accelerating voltage of 5 kV.

X-ray diffractograms, were recorded in a Siemens D-501 equipment, with a Bragg–Brentano configuration, using Cu$K\alpha$ ($\lambda = 1.5418$ Å). Spectra were collected in the range $2\theta = 20°$–$80°$, with a step of 0.05° and an acquisition time of 1 s for each point.

2.5. Catalytic activity tests

Reaction was carried out in a fixed-bed tubular reactor ("U" shaped), using 20 mg of catalysts between two pompons of quartz wool. The CH_4 and CO_2 or H_2O reactants were mixed at a ratio of 1 diluted in He (10:10:80 in volume). The gas hourly space velocity (GHSV) was 300,000 L/kg h. In the case of $CH_4 + H_2O$ reaction, a Fresenius "Orchestra" perfusor was used for injecting the water onto the CH_4 + He mixture, being all the pipes from this point up to chromatograph heated at 65 °C. Samples were heated from room temperature up to 750 °C at 1 °C/min rate, holding the samples at 750 °C during 17 h, and cooled down to room temperature in the same reaction mixture.

Reactives and products were analyzed using a gas chromatograph (Varian, GC-3800) with a thermal conductivity detector (TCD), and two columns with an "in line" configuration (Molecular Sieve 5 Å, Porapak ®-N).

2.6. X-ray absorption spectroscopy

X-ray absorption spectra (XAS) were recorded at the BM25 beam line (SPLINE) of the ESRF synchrotron (Grenoble, France). The spectra were acquired in transmission mode with a modified commercial infrared cell (Specac), using self-supported wafers of the Ni–ceria sample. In all cases, XAS spectra were collected at 600, 750 °C and finally, after cooling down to RT. In all cases the pellets were prepared using the optimum weight to maximize the signal-to-noise ratio in the ionization chambers ($\log I_0/I_1 \approx 1$). Mass flow controllers were used for dosing the gases to the cell, using a total flow of 100 ml/min. The composition of the gas mixtures were similar to that previously used in the TPR experiment, for the hydrogen reduction treatment, and in catalytic test, for the reforming reaction experiments. For energy calibration, a standard Ni foil was introduced after the second ionization chamber (I_1) and measured simultaneously. Typical XAS spectra of NiK edge were recorded from 8025 to 9000 eV, with a variable step energy value, with a minimum 0.5 eV step across the XANES region. Once extracted from the XAS spectra, the EXAFS oscillations were Fourier transformed in the range 2.4–11.0 A^{-1}. Spectra were analyzed using the software package IFEFFIT [14]. The theoretical paths for Ni–Ni and Ni–O species used for fitting the first coordination shell of the experimental data were generated using the FEFF 7.0 program [15]. The coordination number, interatomic distance, Debye–Waller factor and inner potential correction were used as variable parameters for the fitting procedures. In order to take in account the anharmonic vibrations of atoms at high temperature, leading to an anharmonic distribution in the instantaneous bond length [16], higher cumulants (third and fourth) were also intended as fitting parameters, which show, respectively, the asymmetry and broadening of the radial distribution function around the adsorbing atom. The use of the third cumulant affects just slightly the values previously obtained for the other parameters. However, the fourth cumulant could not be used in the fitting procedure because its introduction as a parameter give unstable fits within each series of experiments with, in some cases, very high and unrealistic coordination numbers and Debye–Waller factors. Reference spectra for metallic Ni and NiO were recorded using standard reference samples.

2.7. Ambient pressure photoemission spectroscopy (APPES)

X-ray photoemission experiments have been carried out under near-ambient pressure conditions in the beamline 9.3.2. at the advanced light source (ALS) of Lawrence Berkeley Laboratory [17]. The Ni/CeO_2 sample was reduced in situ with hydrogen at 500 °C, exposed to the gas mixture (about 1 Torr of methane and/or CO_2), and gradually heated up to 650 °C. The equipment, provided with a differentially pumped lenses system, permits the evaluation of photoelectrons ejected from the sample surface species at this relatively high pressure. Typical scattering problems in the presence of high-pressure gas atmospheres can be overcome and valuable information about the surface-mechanism interaction between catalyst and gas reactants can be elucidated [17].

3. Results and discussion

3.1. Characterization of the catalyst

The 26 wt% Ni/CeO_2 sample calcined at 750 °C for 2 h has a BET surface of 16 m^2/g. The XRD obtained after calcination is displayed in Fig. 1. As previously found for other Ni/ceria catalysts [10], it shows peaks characteristics of the cubic structures of both, CeO_2 and NiO, with no other phases detected by this technique. By applying the Scherrer equation, the size of the NiO particles have been estimated to be around 10 nm, which agrees with the estimation from the SEM images of this sample, included in Fig. 2. As shown in these images, after calcination, the synthesized Ni–ceria catalyst is composed by big irregular particles, of about 1 μm in size, sprinkle on the surface with very homogeneous cubic-shape particles. The energy-filtered analysis of these images allows us to assign the larger particles to the CeO_2 phase, and the tiny cubic ones to a well dispersed NiO phase. Because the relatively high content of nickel in this sample and the preparation method used, some others NiO particles must be likely located in subsurface regions of the cerium oxide. This has been confirmed by quantifying the Ce 3d and Ni 2p XPS signal obtained for the sample after calcination (not shown). The surface composition has proved to be the same as the nominal of the catalyst, showing that nickel is homogeneously distributed on all the ceria particles.

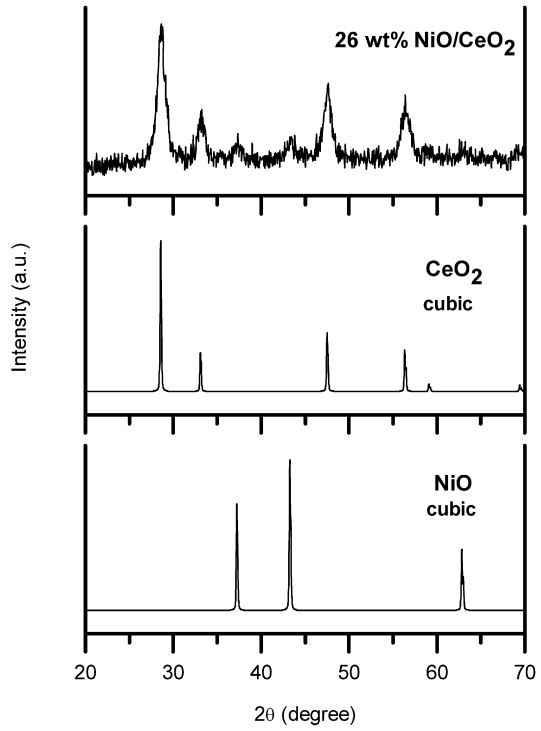

Fig. 1. XRD diagram of the 26 wt% NiO/CeO_2 sample after calcination at 750 °C.

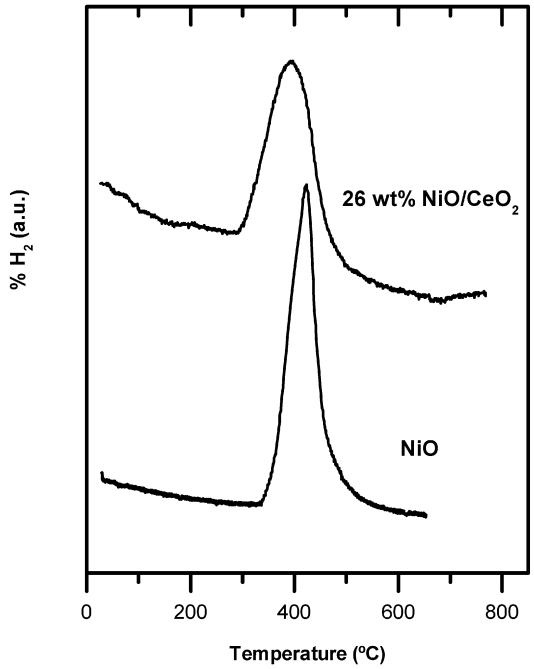

Fig. 3. Temperature-programmed reduction (TPR) profile of the 26 wt% NiO/CeO_2 sample after calcination at 750 °C.

According to the data obtained by temperature programmed reduction, included in Fig. 3, these nanoparticles are slightly more reducible than a massive NiO, also included in the figure as a reference. As determined by the quantitative calculation of the hydrogen consumption at 600 °C, the nickel is completely reduced to Ni(0) at this temperature.

3.2. Catalytic activity in the reforming reactions of methane

The catalytic activity of the Ni/CeO_2 system was determined for the steam and dry reforming reactions of methane using an GHSV of 3×10^5 L/kg h. As shown in Fig. 4, the catalyst is initially much more active for the steam reforming reaction, but the activity drops almost linearly with time on stream. However, the catalytic activity in CO_2 reforming, although initially lower, is pretty much stable after 300 min on reaction. It is generally accepted that the metal phase are directly responsible for carbon deposition and deactivation processes [18,19]. Also, these two reactions, dry and steam reforming of methane, have been found to be mechanistically similar [20]. So, and according to previous results with ceria supported catalysts [21], such a better stability in the more demanding dry reforming reaction, must be related with differences

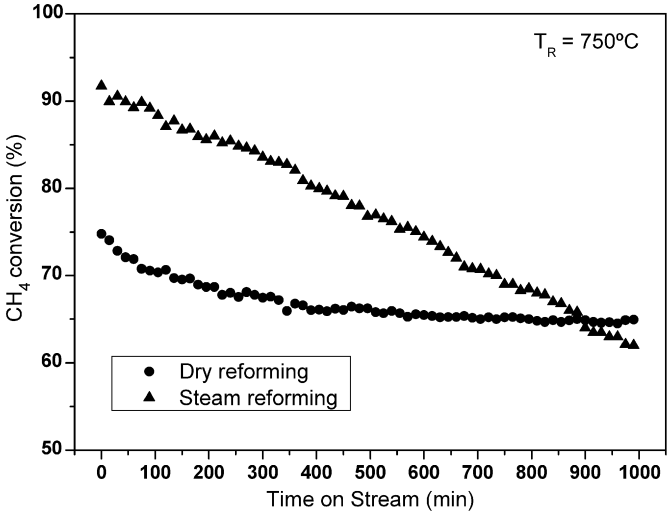

Fig. 4. Evolution of methane conversion with time of stream for dry and steam reforming of methane at 750 °C. Catalyst = 0.02 g. GHSV = 3×10^5 L/kg h. BET surface area = 16 m^2/g.

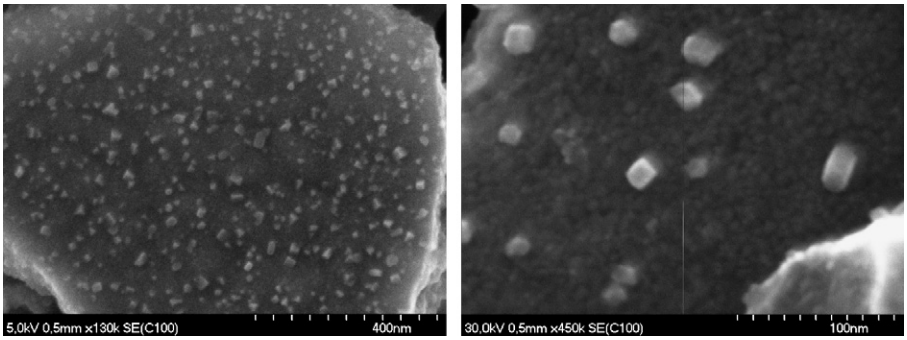

Fig. 2. SEM pictures of the 26 wt% NiO/CeO_2 sample after calcination at 750 °C.

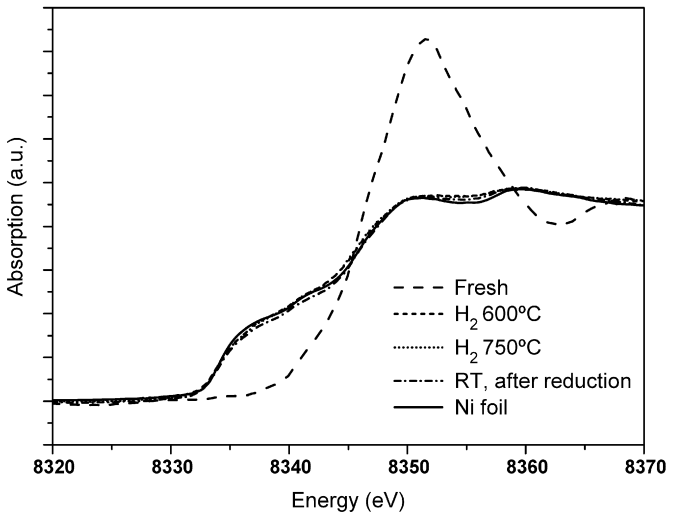

Fig. 5. In situ XANES spectra of the 26 wt% NiO/CeO_2 sample submitted to H_2 reduction treatment at the indicated conditions. All the spectra have been collected in contact with the gas phase.

in the interaction between nickel and ceria when in contact with the CH_4/H_2O and CH_4/CO_2 mixtures, respectively.

3.3. In situ XAS study of reduction

The physico-chemical state of nickel during the reduction pretreatment and the steam and dry methane reforming reactions has been monitored by means of in situ XAS spectroscopy. In all treatments, spectra were collected in situ at 600, 750 °C and, finally, after cooling down to room temperature.

The XANES spectra obtained during the reduction treatment with hydrogen, included in Fig. 5, present white lines and pre-edge similar to the Ni foil used as a reference, showing that the original NiO phase is completely reduced to Ni(0) at 600 °C [22], which is also in agreement with the previous TPR measurements (Fig. 3). The spectra obtained during the treatments at 750 °C in hydrogen and the subsequent collected after cooling down to RT in hydrogen are also similar to that of the Ni foil, included in the figure as a reference. The light differences between the XANES spectra of the reduced samples at high and room temperature can be ascribed to the higher thermal disorder at 600 and 750 °C, toning down the intensity of the oscillations. This behavior is slightly different to that found by Dull et al. in a highly dispersed Ni-MCM-41 catalyst [23], which is not completely reduced after a similar reduction treatment. In our case, the 10 nm NiO particles show the same behavior as a massive NiO compound reduced at this high temperature.

The EXAFS oscillations extracted from the XAS spectra and the Fourier transformed functions obtained for the hydrogen reduction treatments are presented in Fig. 6. At RT, the Fourier transform (FT) function is similar to that of the metallic reference, confirming the nickel has been completely reduced. The fitting analysis of the main peak at around 2–3 Å in this FT function, corresponding to the first Ni–Ni coordination shell, yields 12 neighbors atoms at 2.49 Å (Table 1). For cubic and spherical particles of around 10 nm in size, less than 20% of atoms are located at the surface [24]. So, the average coordination number for a compact packing arrangement of the atoms in these nanoparticles must be much higher than 11 (C.N. $> 0.2 \times 9 + 0.8 \times 12 = 11.4$; 20% of atoms with a C.N. of 9 (surface) and 80% with a C.N. of 12 (bulk)). Therefore, the value of 12 obtained for these particles is within the estimated error of 10%, and so in agreement with the particle size of about

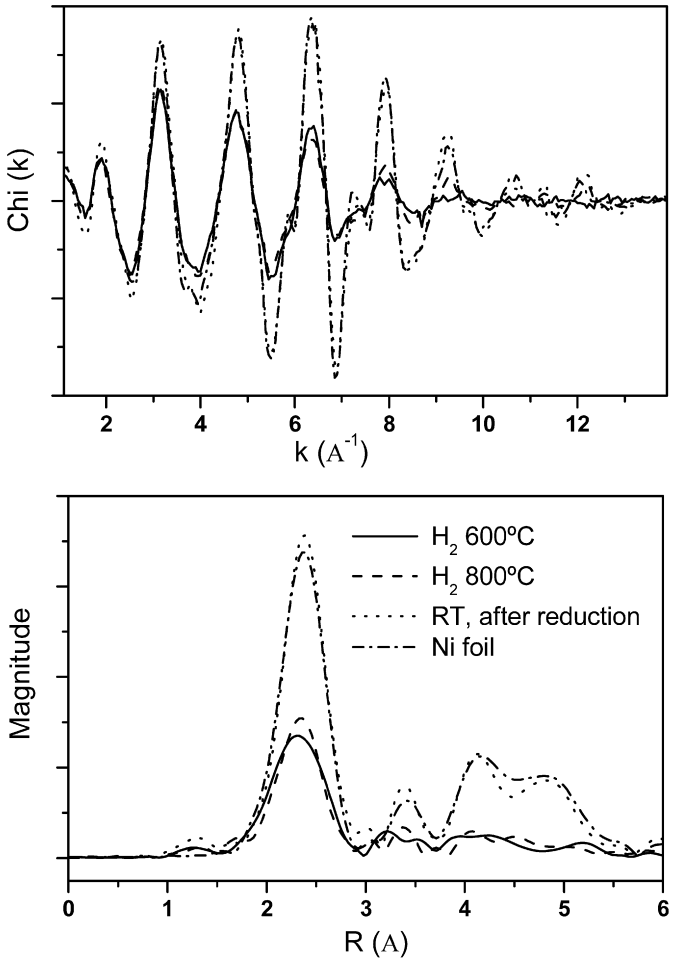

Fig. 6. EXAFS oscillations and Fourier transform functions obtained for the 26 wt% NiO/CeO_2 sample submitted to H_2 reduction treatment at the indicated conditions. All the spectra have been collected in contact with the gas phase.

Table 1
Structural parameters for Ni obtained by fitting analysis of the EXAFS spectra of Ni/ceria catalyst submitted to the indicated treatments

	Ni–Ni (A)	C.N.	D–W ($A^2 \times 10^{-3}$)	ΔE_0 (eV)	3rd cumulant ($A^3 \times 10^{-4}$)
H_2 600 °C	2.49	12.3	16	−6.3	5.3
H_2 750 °C	2.48	9.7	12	−6.7	1.6
H_2 RT	2.49	12.0	6	−5.2	0.6
$CH_4 + H_2O$ 600 °C	2.49	12.7	15	−5.5	7.1
$CH_4 + H_2O$ 750 °C	2.50	12.7	19	−4.8	14.8
$CH_4 + H_2O$ RT	2.05 (Ni–O)	0.5	2	8.5	–
	2.50 (Ni–Ni)	10.9	7	−2.3	3.5
$CH_4 + CO_2$ 600 °C	2.49	12.6	16	−6.7	2.9
$CH_4 + CO_2$ 750 °C	2.48	7.5	10	−5.7	0.6
$CH_4 + CO_2$ RT	2.49	10.7	5	−4.2	2.4
Ni foil	2.48	12.0	5	−6.0	−0.4

Note. Estimated errors: interatomic distance, $< \pm 0.02$ A; coordination number (C.N.), $< \pm 10\%$.

10 nm previously deduced from XRD and SEM for the original NiO phase.

More interesting is the information obtained from the reduction treatments at 600 and 750 °C. So, although the FT obtained at 600 °C is much smaller than that obtained at RT, the calculated structural parameters show no significance differences between the metal particles in these conditions and those obtained at RT (Table 1). The main difference lies on the Debye–Waller factors, higher at 600 °C, in agreement with the higher thermal disorder at these conditions. However, the FT obtained during the

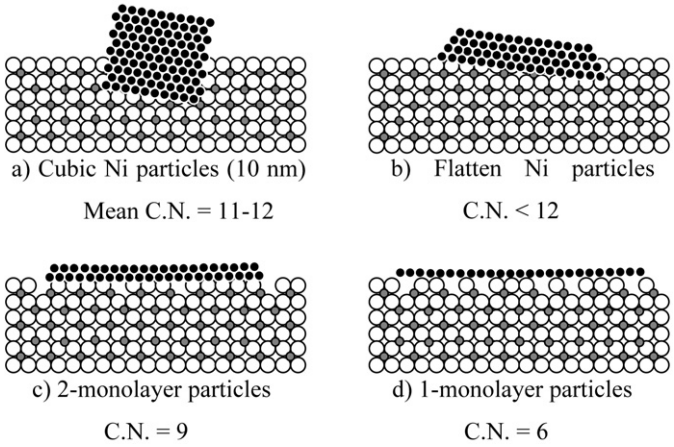

Scheme 1. Schematic evolution of the shape of the metallic nickel particles submitted to a reducing treatment up to 750 °C. By high temperature reduction, the nickel spread onto the partially reduced surface of ceria. The mean coordination number of nickel strongly depends on the shape: from >11 for the cubic 10 nm particles (a) to 9 for the two monolayer particles (c) and 6 for the one monolayer particles (d).

hydrogen treatment at 750 °C has a taller and narrower main peak (2–3 Å) which, in accordance with the structural parameters obtained by mathematical fitting, comes from the formation of smaller but slightly more ordered particles of metallic nickel, as shown, respectively, by a lower Ni–Ni coordination number (9.7 vs 12.3 at 600 °C) but also by a lower Debye–Waller factor (0.012 vs 0.016 A^2). It is worthy of noting here that the third cumulant values do not evolve either linearly with temperature, decreasing between 600 and 750 °C, contrary to what has been previously found for other catalytic systems [16]. These unexpected results, showing that at this high temperature in hydrogen a new nickel phase must be likely stabilized on the ceria surface, could be related with the reducibility of the Ce(IV) to Ce(III) species at this high temperature and the subsequent mobility of oxygen species, a well-known feature specially favored on the ceria surface [21,25]. This effect of ceria modifying the state of the nickel particles, that can be considered as part of the so-named strong metal–support interaction (SMSI) has been recently considered by other authors [26]. Our results could indicate that the reduced ceria surface allows the formation of new nickel particles spreading on the partially reduced ceria support, which could account for a lower value in the mean coordination number. However, a mere change in the particle shape, for instance from cubic to spherical, could not account for this decrease, as the lesser number of atoms in the surface of rounded particles would imply a higher average coordination number. So, only the breakage of the particles or more likely, the formation of flattened particles, as sketched in Scheme 1, induced by a strong interaction between the nickel and the reduced ceria support, could account for the observed decrease in the coordination number. Also, the intimate contact between the nickel particles and the ceria support, required for the stability of these flattened particles, could explain the decreasing in the Debye–Waller factor when the temperature is increased. It is important to note that, in any case, the fitting cannot be improved by adding a second coordination shell of Ni–O, that confirming the nickel is completely reduced, and no support effect could be detected in the oxidation state of nickel. Finally, as mentioned before, after cooling down to RT in hydrogen, the structural parameters of nickel particles are restored, showing that this special interaction between nickel and ceria is only feasible at very high temperature. To our knowledge, this kind of morphological changes has not been previously reported in these sort of catalytic systems under reduction conditions. However, van't Blik et al. [27] found previously changes in the shape of Rhodium particles supported on alumina, when

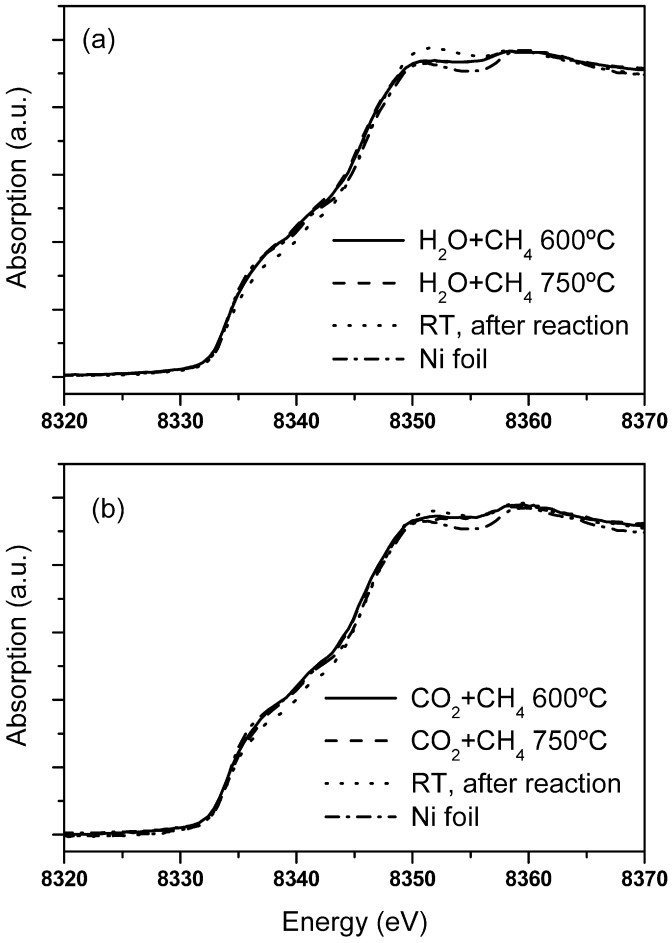

Fig. 7. In situ XANES spectra of the 26 wt% NiO/CeO_2 sample submitted to methane reforming reactions at the indicated conditions. (a) Steam reforming reaction. (b) Dry reforming reaction. All the spectra have been collected in contact with the gas phase.

submitted to CO treatments. Also, Newton et al. have recently published some interesting results in relation with shapes changes occurring in Pd catalysts under CO/NO exposures [28]. These authors have detected by in situ XAS a reversible redispersion and sintering of Pd nanoparticles over a ceria–zirconia–alumina support at 673 K. In our case, the driving force for the shape modifications can be certainly assigned to a special kind of interaction with the ceria support, only achievable at strong reducing conditions.

3.4. In situ XAS study during catalytic reactions

The Ni/CeO_2 sample has also been studied by in situ XAS during steam and dry reforming reaction of methane at 600 and 750 °C. The XANES regions of the spectra are included in Fig. 7 for both reforming reactions, where no significances differences can be observed, except for the spectrum collected at room temperature after the steam reforming reaction. In this case, a slightly more intense white line can be detected, while the rest of them are in keeping with the presence of a well reduced Ni phase. In spite of the mild oxidizing properties of CO_2 [18], the nickel particles remain completely reduced during all the dry methane reforming treatments, and only in the presence of water, a more powerful oxidant, are the nickel particles partially oxidized at RT. No peaks from nickel carbides or similar species were detected during the reaction treatments, which, according to Takenaka et al. [29] would produce changes in the low energy region of the XANES spectra (8330–8340 eV).

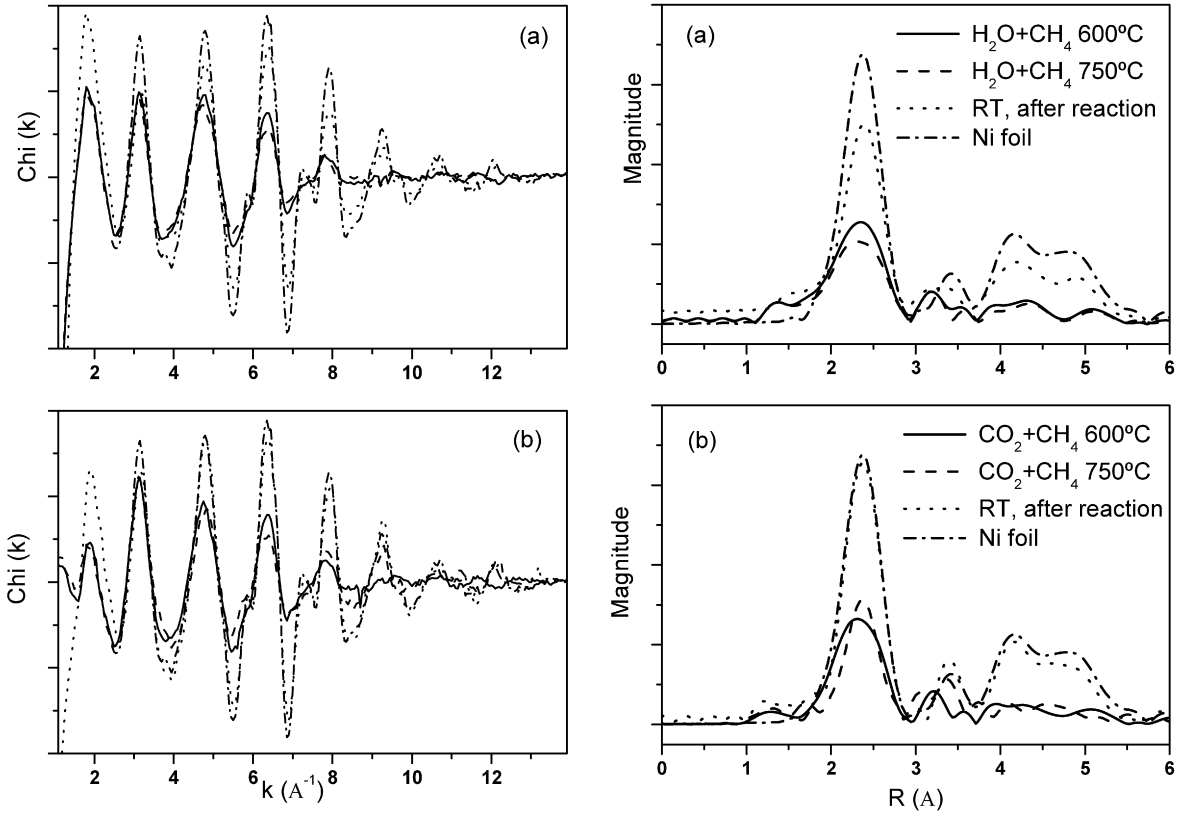

Fig. 8. EXAFS oscillations and Fourier transform functions obtained for the 26 wt% NiO/CeO_2 sample submitted to methane reforming reactions at the indicated conditions. (a) Steam reforming reaction. (b) Dry reforming reaction. All the spectra have been collected in contact with the gas phase.

The oscillations and FT functions of the EXAFS regions of the XAS spectra during the reforming reaction treatments are included in Fig. 8. During the steam reforming reaction at 600 and 750 °C the fitting analysis accomplished for the first coordination shell (Fig. 8a, Table 1) show at both temperatures that, in contact with the water/methane mixture, the Ni particles remaining basically unchanged, with a coordination number around 12 and a Debye–Waller factor increasing as the temperature does it, which is liable for the lower intensity of the FT main peak as the temperature increases. Also, now the third cumulant values go up as the temperature is increased, with a top value of 0.0015 A^3 at 750 °C. It is worthy to note that this behavior is different to that observed previously during reduction (Fig. 6), and so, these findings support the assumption that, for the change in the size and morphology of the nickel particles to occur, the ceria support must be partially reduced, which can not be accomplished in contact with the less reducing water/methane mixture. Finally, when the sample is cooled down to RT, the intensity of the main peak is not completely recovered under the water/methane mixture. The parameters obtained by fitting analysis show the presence of metallic particles similar in size to the original ones (C.N. = 11.3) but the nickel particles are now partially oxidized, as indicated by the Ni–O contribution at 2.05 A. Although with a very low coordination number (C.N. = 0.5), this Ni–O contribution could not be introduced in the other treatments, being also in agreement with the slightly higher white line of the XANES spectrum obtained in these conditions (Fig. 7). It is important to note that due to the weakness of this Ni–O contribution, it was not feasible the use of the third cumulant for this Ni–O shell which gave unrealistic parameters. Again, no contributions from nickel carbides were detected by fitting analysis.

Interestingly, the behavior of the nickel particles under dry methane reforming conditions is similar to that observed previously during hydrogen reduction, and therefore different for the previous described under steam reforming. The analysis of the EXAFS functions obtained under these reactions conditions is included in Fig. 8b and Table 1. Now, the metallic phase exposed to the CO_2/methane mixture at 600 °C has similar structural parameters to that obtained previously under hydrogen and steam reforming conditions. However, by increasing the temperature up to 750 °C, a narrower main peak can be observed in the FT (Fig. 8b), and again the structural parameters obtained by fitting (C.N. = 7.5 and D–W = 0.010 A^2), indicate that the metallic phase has been modified in size and/or morphology by heating at this high temperature. Again, the higher value for the third cumulant has been obtained at 600 °C, decreasing when the temperature go up to 750 °C. In this case, the parameters are only partially recovered after cooling down to RT, which, as it will be shown below in more details, could reflect the effect of the carbon deposits protecting and blocking the metallic particles.

Fig. 9 shows a detailed representation of the main peak in the FT functions obtained at 600 and 750 °C during the different treatments: hydrogen reduction, steam and dry reforming of methane. As it can be observed, the main FT peaks at about 2.4 Å (without phase correction) obtained at 600 °C in the three different treatments have maxima lying in an intermediate position of intensity. At 750 °C, the peak obtained under steam reforming reaction conditions is clearly less intense, as could be expected for just an increase in the D–W factor when increasing the temperature. However, the behavior in the other cases, hydrogen reduction and dry reforming reaction, is opposite. This change in the peaks intensities and widths must be related with a real modification in the structure of the metallic particles under strong enough reducing conditions, as those fulfilled in contact with hydrogen or the methane/CO_2 mixture. It is worthy to note that this change in morphology, graphically represented in Scheme 1, could explain the higher stability of the Ni/CeO_2 catalyst in the dry reform-

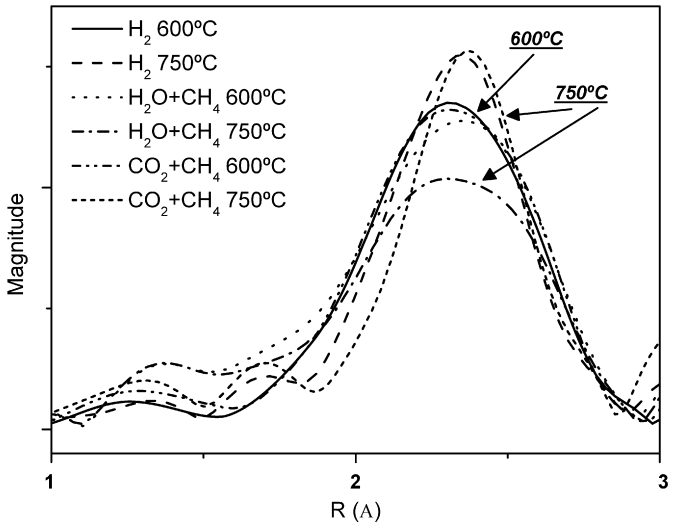

Fig. 9. Detailed Fourier transform functions (1–3 A) of the EXAFS region of the 26 wt% NiO/CeO_2 sample submitted to treatments at 600 and 750 °C.

ing reaction (Fig. 4). According to Wei and Iglesia [30], the rate-determining step of both the methane reforming reaction and the formation of carbon deposits are the dissociative absorption of the hydrocarbon on the metal. Highly unsaturated nickel atoms have a higher reactivity for this dissociative step, which are also the most active sites for carbon formation [31]. Selective blocking of these sites, less likely in Ni(111) surfaces, could hinder preferably the carbon nucleation process. This has been intended previously in several ways, as introducing sulfur compounds in the gas mixtures or alloying the nickel with metals as gold, which is supposedly preferentially located at the most unsaturated sites of the nickel particles [31–33]. In our Ni/CeO_2 catalytic system, the formation of flattened nickel particles at high temperature as a consequence of a SMSI effect, could account for the higher stability of the catalyst under dry reforming reaction conditions, as the number of unsaturated nickel atoms decreases with this morphology.

3.5. In situ APPES study during dry reforming reaction

Some of the resemblances and differences in the behavior of the Ni/CeO_2 catalyst at 750 °C during hydrogen reduction and reforming reactions of methane can be clarified from the results obtained by in situ APPES spectroscopy under dry methane reforming conditions at 650 °C, the higher achievable temperature. Fig. 10 includes the Ce 4d region spectra obtained for different treatments at this temperature. The fresh sample presents a complex spectra similar to that previously reported for the Ce(IV) species of CeO_2 [34], which remains unchanged by treatment with a CO_2/methane mixture at the same temperature (not included). As the temperature could not be increased due to technical limitations, the redox properties of the ceria were checked by submitting the catalyst to a treatment with pure methane at the same temperature, which produces important changes in the profile of the Ce 4d spectra. According to the previous work of Mullins [34], these changes in the very complex Ce 4d signal are due to the complete reduction of the ceria surface to Ce(III) species. Therefore, this confirms that under reduction conditions at high temperature the ceria surface undergoes important chemical changes, which could induce modifications in the nickel particles supported on it, as those observed in this work. Surprisingly, after a subsequent treatment with CO_2 at 650 °C, the original signal is not completely recovered, indicating that a mixture of Ce(III) and Ce(IV) species are formed in the surface of the support. This resistance to be

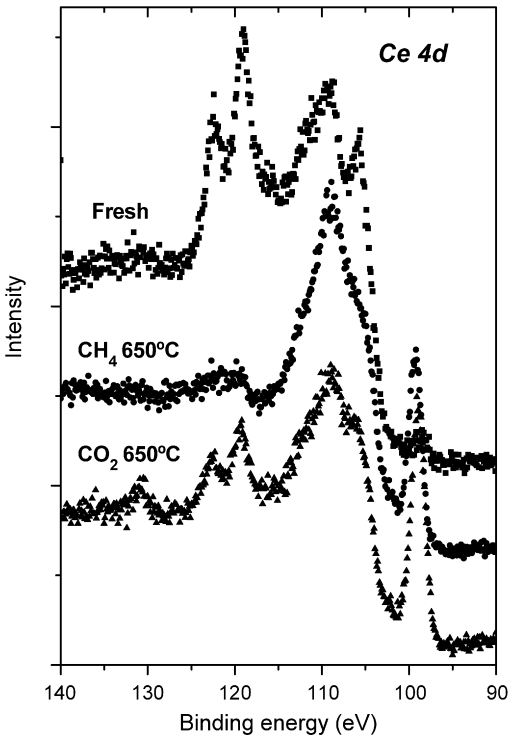

Fig. 10. Ce 4d APPES spectra of the 26 wt% NiO/CeO_2 sample submitted to different treatments at 650 °C. All the spectra have been collected in contact with the gas phase. (Peak around 99 eV corresponds to Si 2p from the sample holder.)

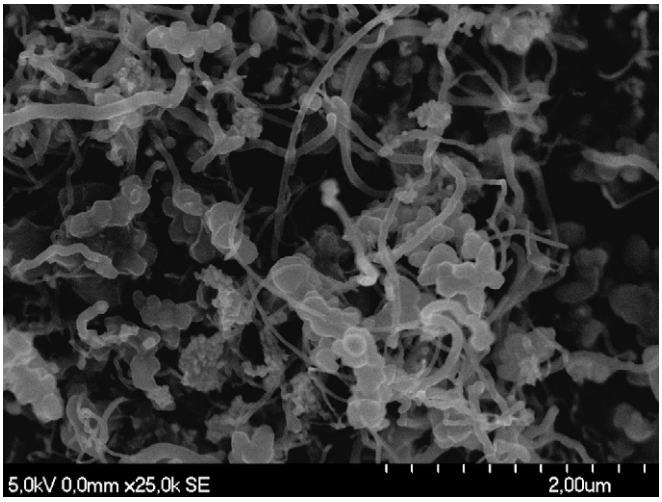

Fig. 11. SEM image of the 26 wt% NiO/CeO_2 sample after dry reforming of methane at 750 °C.

oxidized could be explained considering the protecting effect of the carbon deposits built on the catalyst during reaction, this preventing its quick oxidation to Ce(IV). These carbon deposits can be observed in the SEM images obtained for this catalyst after dry methane reforming reaction (Fig. 11), where no individual particles of metallic nickel could be detected. Nevertheless, it is interesting to note that the size of the carbon nanofibers observed by SEM (around 100 nm) is much higher than the 10 nm size of the original metallic particles. As these fibers are formed from the nickel particles, this large size could be related with the large exposed size of the flattened particles of nickel on the ceria support. In any case, as said before, no metal particles have been detected by SEM after the dry reforming reaction. Moreover, these layers of carbon could account for not only the higher stability of Ce(III) to be reox-

idized by CO_2, but for the different behavior of the nickel particles after cooling down to RT which, contrary to that observed previously in hydrogen, under CO_2/methane maintain a coordination number clearly lower than 12.

4. Conclusions

The steam and dry reforming reactions of methane have been carried out over a Ni/CeO_2 powder sample prepared by combustion synthesis. This catalytic system is composed by 10 nm cubic NiO particles, homogeneously distributed on the ceria support. Also, it presents a good performance for both steam and dry reforming reactions of methane. In situ XAS analysis has revealed that the metallic nickel formed by hydrogen reduction is not oxidized under reaction conditions. Only after cooling down to RT in the steam reforming mixture (CH_4/H_2O), the nickel particles are slightly oxidized. The in situ study has shown that, in contact with hydrogen or the CH_4/CO_2 mixture at 750 °C, the morphology and size of the nickel particles evolve likely to a flattened shape, spreading over the partially reduced ceria support, and been stabilized by a strong interaction between the metal and the partially reduced ceria support (SMSI). The formation of flattened particles, having less unsaturated metal sites, could account for the higher stability observed under dry reforming reaction compared to the reforming with water. This shape is only stable at high temperature or, as is the case in the catalyst submitted to dry reforming conditions, when particles are partially covered by carbon deposits. These deposits also prevent a quick oxidation of the Ce(III) species when exposed to CO_2 at high temperature.

Acknowledgments

We thank the Ministry of Science and Education of Spain for financial support (Projects ENE2004-01660 and ENE2007-67926-C02-01). We also thank the staff of the ESRF BM25 beamline, the staff of the ALS 9.3.2 beamline and to Dr. M.Salmeron (LBL, Berkeley) for discussions and help related with the APPES technique.

References

[1] J.N. Armor, Appl. Catal. A 176 (1999) 159.
[2] M.A. Peña, J.P. Gomez, J.L.G. Fierro, Appl. Catal. A 144 (1996) 7.
[3] Editorial, Int. J. Hydr. Energy 27 (2002) 721.
[4] J.O.M. Bockris, Int. J. Hydr. Energy 27 (2002) 731.
[5] M.C.J. Bradford, M.A. Vannice, Catal. Rev. Sci. Eng. 41 (1999) 1.
[6] D. Lee, P. Hacarlioglu, S.T. Oyama, Top. Catal. 29 (2004) 45.
[7] Y. Matsumura, T. Nakamori, Appl. Catal. 258 (2004) 107.
[8] D.K. Kim, K. Stowe, F. Muller, W.F. Maier, J. Catal. 247 (2007) 101.
[9] P. Kumar, Y. Sun, R.O. Idem, Energy Fuels 21 (2007) 3113.
[10] S. Xu, X. Yan, X. Wang, Fuel 85 (2006) 2243.
[11] A. Trovarelli, C. Leitenburg, J. Llorca, G. Dolcetti, J. Catal. 151 (1995) 111.
[12] A. Civera, M. Pavese, G. Saracco, V. Specchia, Catal. Today 83 (2003) 199.
[13] P. Malet, A. Caballero, J. Chem. Soc. Faraday Trans. I 84 (1988) 2369.
[14] M. Newville, J. Synchrotron Rad. 8 (2001) 322.
[15] A.L. Ankudinov, J.J. Rehr, Phys. Rev. B 56 (1997) R1712.
[16] E. Bus, J.T. Miller, A.J. Kropf, R. Prins, J.A. van Bokhoven, Phys. Chem. Chem. Phys. 8 (2006) 3248.
[17] F.D. Ogletree, H. Bluhm, G. Lebedev, C.S. Fadley, Z. Hussain, M. Salmeron, Rev. Sci. Instrum. 73 (2002) 3872.
[18] J.H. Bitter, K. Seshan, J.A. Lercher, J. Catal. 176 (1998) 93.
[19] K. Takanabe, K. Nagaoka, K. Nariai, K. Aika, J. Catal. 230 (2005) 75.
[20] J.R. Rostrup-Nielsen, J.H.B. Hansen, J. Catal. 144 (1993) 38.
[21] T. Huang, H. Lin, T. Yu, Catal. Lett. 105 (2005) 239.
[22] Y. Yang, S. Lim, G. Du, Y. Chen, D. Ciuparu, G.L. Haller, J. Phys. Chem. B 109 (2005) 13237.
[23] G. Du, S. Lim, Y. Yang, C. Wang, L. Pfefferle, G.L. Haller, J. Catal. 249 (2007) 370.
[24] K.J. Klabunde, J. Stark, O. Koper, C. Mohs, D.G. Park, S. Decker, Y. Jiang, I. Lagadic, D. Zhang, J. Phys. Chem. 100 (1996) 12142.
[25] J.B. Wang, Y.S. Wu, T.J. Huang, Appl. Catal. A 272 (2004) 289.
[26] S.M. Lima, J.M. Assaf, M.A. Peña, J.L.G. Fierro, Appl. Catal. A 311 (2006) 94.
[27] H.F.J. van't Blik, J.B.A.D. van Zon, T. Huizinga, J.C. Vis, D.C. Koningsberger, R. Prins, J. Am. Chem. Soc. 107 (1985) 3139.
[28] M.A. Newton, C. Belver-Coldeira, A. Martinez-Arias, M. Fernandez-Garcia, Nature Mater. 6 (2007) 528.
[29] S. Takenaka, Y. Shigeta, E. Tanabe, K. Otsuka, J. Phys. Chem. B 108 (2004) 7656.
[30] J. Wei, E. Iglesia, J. Catal. 224 (2004) 370.
[31] H.S. Bengaard, J.K. Norskov, J. Sehested, B.S. Clausen, L.P. Nielsen, A.M. Molenbroek, J.R. Rostrup-Nielsen, J. Catal. 209 (2002) 365.
[32] F. Besenbacher, I. Chorkendorff, B.S. Clausen, B. Hammer, A.M. Molenbroek, J.K. Norskov, I. Stensgaard, Science 279 (1998) 1913.
[33] Y. Chin, D.L. King, H. Roh, Y. Wang, S.M. Heald, J. Catal. 244 (2006) 153.
[34] D.R. Mullins, J. Electr. Spec. Rel. Phenom. 114 (2001) 333.